Linear gain of a free-electron laser with an electromagnetic wiggler and an axial-guide magnetic field

H. P. Freund
Science Applications International Corporation, McLean, Virginia 22102

R. A. Kehs* and V. L. Granatstein
University of Maryland, College Park, Maryland 20742
(Received 31 March 1986)

The small-signal gain for an electromagnetically pumped free-electron laser is calculated for an amplifier configuration which includes an axial-guide magnetic field. The large-amplitude electromagnetic wave acts like the magnetostatic wiggler in a conventional free-electron laser, and the expression for the gain is shown to reduce to the well-known result in the limit of a magnetostatic wiggler. Substantial enhancements in the gain are found when $\Omega_0 \simeq \gamma_0(\omega_w + k_w v_{||})$, where Ω_0 is the axial gyrofrequency, γ_0 is the relativistic factor for the electron beam, $v_{||}$ is the axial velocity of the electron beam, and (ω_w, k_w) are the frequency and wave vector of the electromagnetic wiggler.

I. INTRODUCTION

A great deal of attention has been focused on the two-stage free-electron-laser (FEL) configuration in recent years due to the potential for short-wavelength operation using electron beams of relatively modest energy. In its most general form, the first stage of the device is used to generate a large-amplitude electromagnetic wave which is employed as a second-stage electromagnetic wiggler. The output wavelength for an electromagnetic wiggler having a wavelength λ_w is given by

$$\lambda = \frac{\lambda_w}{(1+\beta_z)^2\gamma_z^2} ,$$

where $\beta_z = v_z/c$ (v_z denotes the axial electron-beam velocity), and $\gamma_z = (1-\beta_z^2)^{-1/2}$. This contrasts with the output wavelength of an FEL using a magnetostatic wiggler of the same period

$$\lambda = \frac{\lambda_w}{(1+\beta_z)\beta_z\gamma_z^2} ,$$

which produces radiation at approximately twice the wavelength as that for an electromagnetic wiggler when $\beta_z \lesssim 1$. A recent experiment using a backward wave oscillator as a first stage in the generation of a large-amplitude electromagnetic wave has demonstrated the feasibility of the concept.[1] Indeed, any convenient source of radiation may be used in the first stage, and designs employing a magnetostatically pumped FEL have been discussed for this purpose.[2,3] The advantage of such a configuration over that of a single-stage magnetostatically pumped FEL is that the output wavelength of the two-stage FEL scales as

$$\lambda = \frac{\lambda_w}{(1+\beta_z)^3\beta_z\gamma_z^4} ,$$

where λ_w denotes the period of the first-stage magnetostatic wiggler.

Our purpose in this work is to determine the small-signal gain in the second stage of such a two-stage configuration for an amplifier configuration. In particular, we are concerned with the effect of an axial magnetic field on the interaction, since for many experiments involving intense relativistic electron beams the axial-guide field is necessary in order to confine the beam against the effects of self-field. Theoretical studies of the gain for such configurations have appeared in the literature;[4,5] however, none of these treatments has included a self-consistent treatment of the orbital coupling between the electromagnetic wiggler and the axial-guide fields. Indeed, for magnetostatically pumped FEL's, the presence of an axial-guide field has been shown to result in an orbital instability in the electron trajectories[6] as well as a negative-mass type of instability in the beam space-charge waves.[7]

The present work represents an extension of a previous study of the electron trajectories in combined electromagnetic wiggler and axial-guide field configurations,[8] which is summarized in Sec. II. The nonlinear pendulum equation which describes particle trapping in the ponderomotive potential formed by the beating of the large-amplitude electromagnetic wiggler and the output radiation field is also derived. Section III is devoted to the derivation of the small-signal gain, and a summary and discussion is given in Sec. IV.

II. SINGLE-PARTICLE ORBITS

The configuration of interest consists of a uniform axial-guide magnetic field, $B_0\hat{\mathbf{e}}_z$, and a backwards-propagating electromagnetic wave described by

$$\mathbf{B}_w(z,t) = B_w[\,\hat{\mathbf{e}}_x\cos(k_w z + \omega_w t) + \hat{\mathbf{e}}_y\sin(k_w z + \omega_w t)] \quad (1)$$

and

$$\mathbf{E}_w(z,t)=\frac{\omega_w}{k_w c}B_w[\,-\hat{\mathbf{e}}_x\sin(k_w z+\omega_w t)$$
$$+\hat{\mathbf{e}}_y\cos(k_w z+\omega_w t)]\,, \tag{2}$$

where B_w denotes the amplitude of the wiggler magnetic field, and (ω_w,k_w) describe the frequency and wave vector. Observe that the Poynting flux is directed antiparallel to the x axis for positive ω_w, and that this representation reduces to that of the static, one-dimensional magnetostatic wiggler in the limit of $\omega_w\to 0$.

We shall find it convenient to work in the reference frame rotating with the wiggler, and define the basis vectors

$$\hat{\mathbf{e}}_1=\hat{\mathbf{e}}_x\cos(k_w z+\omega_w t)+\hat{\mathbf{e}}_y\sin(k_w z+\omega_w t)\,,$$
$$\hat{\mathbf{e}}_2=-\hat{\mathbf{e}}_x\sin(k_w z+\omega_w t)+\hat{\mathbf{e}}_y\cos(k_w z+\omega_w t)\,,$$
$$\hat{\mathbf{e}}_3=\hat{\mathbf{e}}_z\,,$$

A class of constant energy, helical trajectories can be found which are of the form[8,9]

$$\mathbf{v}_0=v_w\hat{\mathbf{e}}_1+v_{\|}\hat{\mathbf{e}}_3\,, \tag{3}$$

where $(v_w,v_{\|})$ are constants given by

$$v_w=\frac{\Omega_w(\omega_w+k_w v_{\|})}{k_w[\Omega_0-\gamma_0(\omega_w+k_w v_{\|})]}\,, \tag{4}$$

$$v_{\|}^2+v_w^2=(1-\gamma_0^{-2})c^2\,, \tag{5}$$

and $\Omega_{0,w}\equiv|eB_{0,w}/mc|$. The stability of this class of helical trajectories can be readily determined by perturbation of the Lorentz force equations, and it is found that instability results whenever

$$\bar{\Omega}^2<0\,, \tag{6}$$

where $\bar{\Omega}$ denotes the natural response frequency of the orbital velocity to the perturbation, and

$$\bar{\Omega}^2\equiv\frac{1}{\gamma_0^2}[\Omega_0-\gamma_0(\omega_w+k_w v_{\|})]$$
$$\times\left[\Omega_0\left[1+\frac{v_w^2}{c^2}\frac{(c^2k_w^2-\omega_w^2)}{(\omega_w+k_w v_{\|})^2}\right]-\gamma_0(\omega_w+k_w v_{\|})\right]\,. \tag{7}$$

As expected, the equations characterizing the orbital velocity and the stability criterion reduce to the well-known results[6,10] of the magnetostatic wiggler in the limit as $\omega_w\to 0$.

The solutions of Eqs. (4) and (5) are characterized by two distinct classes of trajectories which, for convenience, we refer to as group I $[\Omega_0<\gamma_0(\omega_w+k_w v_{\|})]$ and group II $[\Omega_0>\gamma_0(\omega_w+k_w v_{\|})]$. Note that for positive (ω_w,k_w), the group I trajectories are always stable for a supraluminous electromagnetic pump, while the group II trajectories are stable for subluminous pumps. In the present case, as in Ref. 8, we assume that the electromagnetic wiggler is supported by the beam. Hence, for a cold (monoenergetic), uniform beam ω_w and k_w satisfy a dispersion equation of the form

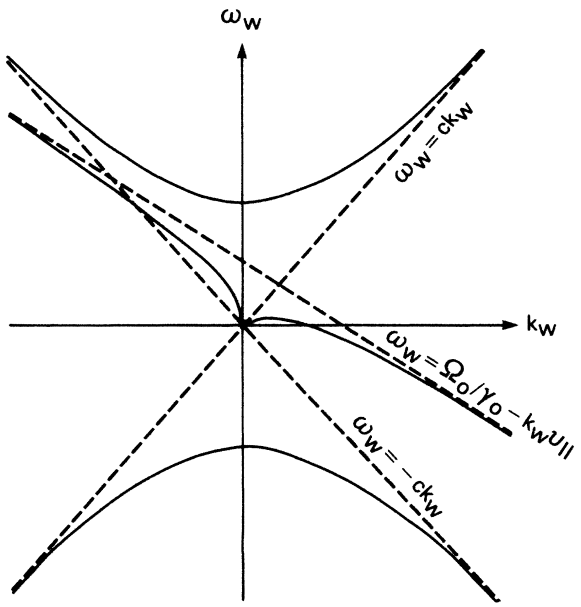

FIG. 1. Schematic illustration of the dispersion characteristics of the backward-propagating electromagnetic wiggler.

$$\omega_w^2-c^2k_w^2-\frac{\omega_b^2(\omega_w+k_w v_{\|})}{\gamma_0(\omega_w+k_w v_{\|})-\Omega_0}=0\,, \tag{8}$$

where $\omega_b^2\equiv 4\pi e^2 n_b/m$ denotes the beam plasma frequency (n_b is the bulk density of the beam). A schematic illustration of the wave modes described by Eq. (8) is shown in Fig. 1. Solution for the orbital velocities, therefore, requires simultaneous solution of Eqs. (4), (5), and (8).

In order to carry the analysis further, we must now specify the particular wave mode of interest. As shown in Fig.1, there are two relevant wave modes for positive (ω_w,k_w): an electromagnetic escape mode and an electromagnetic electron cyclotron wave supported by the

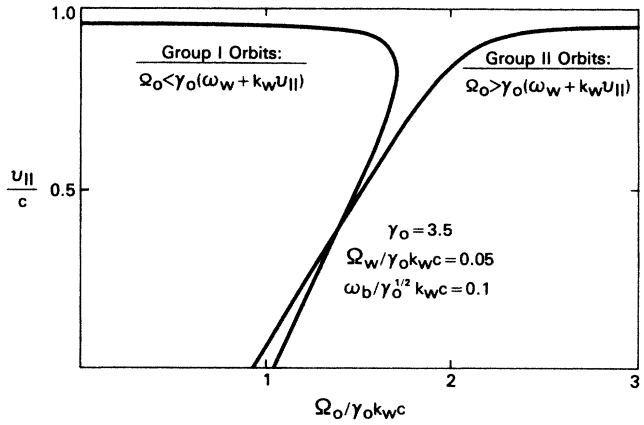

FIG. 2. Graph of the axial velocity versus the axial-guide field for $\Omega_w/\gamma_0 ck_w=0.05$, $\gamma_0=3.5$, and $\omega_b/\gamma_0^{1/2}ck_w=0.1$.

beam. The coupled orbit and dispersion equations are solved numerically for each mode, and the solutions for $v_{\parallel}/c$ versus $\Omega_0/\gamma_0 ck_w$ are shown in Fig. 2 for $\Omega_w/\gamma_0 ck_w=0.05$, $\gamma_0=3.5$, and $\omega_b/\gamma_0^{1/2}ck_w=0.1$. The solutions corresponding to the electromagnetic escape mode are group I orbits which are stable since this mode is supraluminous. In addition, an upper bound on the allowed axial magnetic field occurs which, for the chosen parameters, is given by $\Omega_0/\gamma_0 ck_w \lesssim 1.68$. In contrast, the solutions corresponding to the electromagnetic electron cyclotron wave are group II orbits with $\Omega_0/\gamma_0 ck_w \gtrsim 0.94$. Since the waves are subluminous, these trajectories are also stable.

We now expand the formulation to include the presence of a small-amplitude plane electromagnetic wave propagating antiparallel to the large-amplitude electromagnetic wiggler and parallel to both the axial-guide field and the direction of electron flow, and write the vector potential in the form

$$\delta\mathbf{A}=\delta A[\hat{\mathbf{e}}_x\cos(kz-\omega t)-\hat{\mathbf{e}}_y\sin(kz-\omega t)] , \tag{9}$$

where δA denotes the amplitude and (ω,k) are the frequency and wave vector. The response of the electron beam to this field configuration is determined by the Lorentz force equations

$$\dot{\mathbf{v}}=-\frac{e}{\gamma m}\left[\left[\vec{1}-\frac{1}{c^2}\mathbf{vv}\right]\cdot(\mathbf{E}_w+\delta\mathbf{E})+\frac{1}{c}\mathbf{v}\times(\mathbf{B}_0+\mathbf{B}_w+\delta\mathbf{B})\right] , \tag{10}$$

and

$$\dot{\gamma}=-\frac{e}{mc^2}\mathbf{v}\cdot(\mathbf{E}_w+\delta\mathbf{E}) , \tag{11}$$

where $\vec{1}$ is the unit dyadic, and

$$\delta\mathbf{E}=-\frac{\omega}{c}\delta A[\hat{\mathbf{e}}_x\sin(kz-\omega t)+\hat{\mathbf{e}}_y\cos(kz-\omega t)] ,$$
$$\delta\mathbf{B}=k\delta A[\hat{\mathbf{e}}_x\cos(kz-\omega t)-\hat{\mathbf{e}}_y\sin(kz-\omega t)] . \tag{12}$$

We solve these equations by perturbation about the helical equilibrium described previously, and write $\mathbf{v}=\mathbf{v}_0+\delta\mathbf{v}$ and $\gamma=\gamma_0+\delta\gamma$. As a result, to first order in δA

$$\delta\dot{v}_1=-\frac{1}{\gamma_0}\left[\Omega_0-\gamma_0(\omega_w+k_w v_{\parallel})-\frac{\omega_w}{ck_w}\frac{v_w}{c}\Omega_w\right]\delta v_2+\frac{e}{\gamma_0 mc}\delta A\times\left[\omega\left[1-\frac{v_w^2}{c^2}\right]-kv_{\parallel}\right]\sin\psi , \tag{13}$$

$$\delta\dot{v}_2=\frac{1}{\gamma_0}[\Omega_0-\gamma_0(\omega_w+k_w v_{\parallel})]\delta v_1-\frac{1}{\gamma_0}(\Omega_w+k_w v_w)\delta v_3-\frac{1}{\gamma_0}v_w(\omega_w+k_w v_{\parallel})\delta\gamma+\frac{e}{\gamma_0 mc}\delta A(\omega-kv_{\parallel})\cos\psi , \tag{14}$$

$$\delta\dot{v}_3=\frac{1}{\gamma_0}\Omega_w\left[1+\frac{\omega_w}{ck_w}\frac{v_{\parallel}}{c}\right]\delta v_2+\frac{e}{\gamma_0 mc}\delta A v_w\left[k-\omega\frac{v_{\parallel}}{c^2}\right]\sin\psi , \tag{15}$$

and

$$\delta\dot{\gamma}=-\frac{\omega_w}{k_w c^2}\Omega_w\delta v_2+\frac{e}{mc^2}\delta A\frac{v_w}{c}\omega\sin\psi , \tag{16}$$

where $\psi=(k+k_w)z-(\omega-\omega_w)t$ denotes the electron phase relative to the ponderomotive potential formed by the beating of the two waves. Differentiation of Eq. (14) then yields

$$\left[\frac{d^2}{dt^2}+\bar{\Omega}^2\right]\delta v_2=\frac{e}{\gamma_0 mc}\delta A\sin\psi\left\{\frac{1}{\gamma_0}\Omega_0\left[\omega\left[1-\frac{v_w^2}{c^2}\frac{\omega_w}{\omega_w+k_w v_{\parallel}}\right]-kv_{\parallel}\left[1+\beta_w^2\frac{k_w v_{\parallel}}{\omega_w+k_w v_{\parallel}}\right]\right]-(\omega-kv_{\parallel})(\omega_w+k_w v_{\parallel}+\dot{\psi})\right\} , \tag{17}$$

where $\beta_w\equiv v_w/v_{\parallel}$. Observe that $\bar{\Omega}$ describes the natural response frequency of the electrons to the perturbation, and determines the stability of the helical trajectories. We now assume that the electron phases with respect to the ponderomotive wave are slowly varying (i.e., $\dot{\psi}\simeq 0$) which defines the electron resonance condition

$$\omega\simeq\omega_w+(k+k_w)v_{\parallel} . \tag{18}$$

Operation on Eq. (15) with the second-order differential operator given in Eq. (17) then yields

$$\frac{d}{dt}\left[\frac{d^2}{dt^2}+\bar{\Omega}^2\right]\delta v_3=\frac{e}{\gamma_0\gamma_{\parallel}^2 mc}\delta A\beta_w\bar{\Omega}^2(\omega-\omega_w)\Phi\sin\psi , \tag{19}$$

upon imposition of the resonance condition [Eq. (18)], where

$$\Phi=1-\left[\frac{k_w v_{\parallel}}{\omega_w+k_w v_{\parallel}}\right]^2\left[1+\frac{\omega_w}{ck_w}\frac{v_{\parallel}}{c}\right]^2\times\frac{\gamma_{\parallel}^2\beta_w^2\Omega_0}{\left[1+\frac{v_w^2}{c^2}\frac{(c^2k_w^2-\omega_w^2)}{(\omega_w+k_w v_{\parallel})^2}\right]\Omega_0-\gamma_0(\omega_w+k_w v_{\parallel})} . \tag{20}$$

If the perturbed velocity arises on a slow time scale with the ponderomotive wave and $\dot{\psi}\ll|\bar{\Omega}|$, then we obtain

$$\frac{d}{dt}\delta v_3\simeq\frac{e}{\gamma_0\gamma_{\parallel}^2 mc}\delta A\beta_w(\omega-\omega_w)\Phi\sin\psi . \tag{21}$$

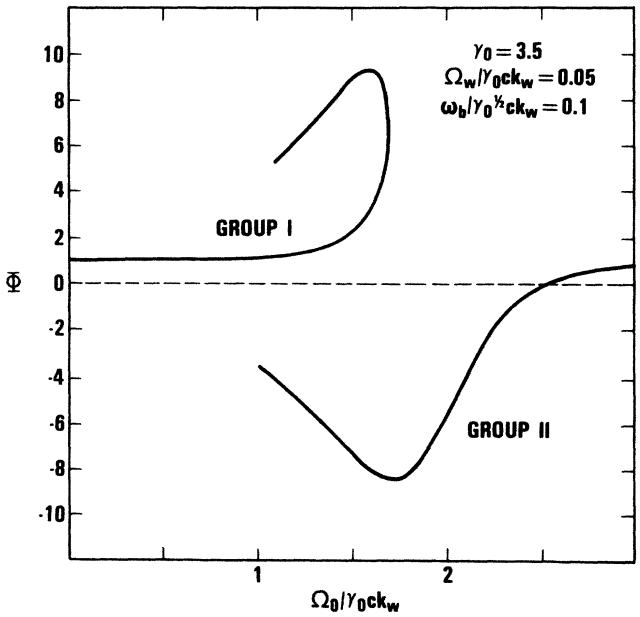

FIG. 3. Graph of Φ versus the axial-guide field for $\Omega_w/\gamma_0 ck_w = 0.05$, $\gamma_0 = 3.5$, and $\omega_b/\gamma_0^{1/2} ck_w = 0.1$.

This approximation is valid as long as the system is not too close to the transition to orbital instability at $\bar{\Omega}^2 = 0$, and is appropriate since the orbits for the system under consideration are stable.

Equation (21) describes a nonlinear pendulum equation for the ponderomotive phase. In order to see this, we note that

$$\frac{d}{dt}\delta v_3 = \frac{1}{k+k_w}\frac{d^2}{dt^2}\psi \simeq \frac{v_{||}^2}{\omega-\omega_w}\frac{d^2}{dz^2}\psi \ , \tag{22}$$

where we express the variation in the phase in terms of the axial position rather than the time, since we are primarily interested in an amplifier configuration. As a result,

$$\frac{d^2}{dz^2}\psi = \frac{(\omega-\omega_w)^2 c}{\gamma_0 \gamma_{||}^2 v_{||}^3}\beta_w \delta a \Phi \sin\psi \ , \tag{23}$$

where $\delta a \equiv e\delta A/mc^2$. Equation (23) describes the axial bunching of the electron beam in the ponderomotive wave. If we note that both v_w and Φ are enhanced near the resonance at $\Omega_0 \simeq \gamma_0(\omega_w + k_w v_{||})$ and that $v_{||}$ decreases, then it is evident that the ponderomotive potential (and, hence, the axial bunching mechanism) may be enhanced due to the presence of the axial-guide field. To illustrate this, we plot Φ versus $\Omega_0/\gamma_0 ck_w$ in Fig. 3 for parameters consistent with the orbits described by Fig. 2.

III. THE SMALL SIGNAL GAIN

The large-amplitude electromagnetic wiggler and the small-amplitude wave are coupled by the presence of the electron beam and, in general, either wave may grow or decay. However, the gain of either wave is proportional to the square of the amplitude of the other mode and we may assume the wiggler field to be constant as long as $\delta B^2 \ll B_w^2$. In the low-gain regime, we may assume that the wave vector k is constant and the amplitude δA is a slowly varying function of the axial position. The evolution of $\delta \mathbf{A}$ is governed by Maxwell's equation

$$\left[\frac{\partial^2}{\partial z^2} - \frac{1}{c^2}\frac{\partial^2}{\partial t^2}\right]\delta\mathbf{A} = -\frac{4\pi}{c}\mathbf{J}_s \ , \tag{24}$$

where the source current is given by[11,12]

$$\mathbf{J}_s = -\frac{en_b v_{z0}}{m}\int_{-\infty}^{\infty} dt_0 \frac{1}{\gamma}\mathbf{p}(t,t_0)W(t_0)\delta[z - z(t,t_0)] \ . \tag{25}$$

In Eq. (25), t_0 is the entry time of the electron (i.e., time at which the electron crossed the $z=0$ plane), $W(t_0)$ is the distribution of entry times, v_{z0} is the initial axial velocity, and $\mathbf{p}(t,t_0)$ and $z(t,t_0)$ are the momentum and axial position at time t of a particle which crossed the $z=0$ plane at time t_0. Observe that a monoenergetic beam is assumed.

For the sake of simplicity, we assume that $\omega \gg \Omega_0, \omega_b$ so that for the tenuous beam, low-gain regime we may write the dispersion relation in the form

$$\omega \simeq ck \ . \tag{26}$$

Defining

$$\tau(z,t_0) = t_0 + \int_0^z dz' \frac{1}{v_z(z',t_0)} \ , \tag{27}$$

the source current may be written as

$$\mathbf{J}_s \simeq -en_b \int_{-\infty}^{\infty} dt_0 W(t_0)\delta[t - \tau(z,t_0)][v_w \hat{\mathbf{e}}_1 + v_{||}\hat{\mathbf{e}}_3] \ . \tag{28}$$

Substituting this form of the source current [Eq. (28)] into Maxwell's equation, we find that

$$2k\frac{d}{dz}\delta a = -\frac{\omega_b^2}{c^2}\frac{v_w}{c}\langle \sin\psi \rangle \ , \tag{29}$$

where the ponderomotive phase is given by

$$\psi = \psi_0 + \int_0^z dz' \left[k + k_w - \frac{\omega-\omega_w}{v_z(z',\psi_0)}\right] \ , \tag{30}$$

$\psi_0 [\equiv -(\omega-\omega_w)t_0]$ is the initial phase, and the average is over the initial phase

$$\langle\theta\rangle \equiv \frac{1}{2\pi}\int_{-\pi}^{\pi} d\psi_0 W(\psi_0)\theta \ . \tag{31}$$

Note that Eq. (31) has been obtained by taking an average over a beat (i.e., ponderomotive) wave period, subject to the assumption that particles entering the interaction region within one beat-wave period execute identical trajectories.[13]

We now assume that the electrons are untrapped by the ponderomotive wave, and seek solutions to Eq. (23) of the form $\psi = \psi_0 + \Delta k z + \delta\psi$, where

$$\Delta k = k + k_w - \frac{\omega-\omega_w}{v_{||}} \tag{32}$$

defines the frequency mismatch. Solution to first order in $\delta\psi$ is straightforward, and we find that

$$\psi=\psi_0+\Delta kz + \frac{(\omega-\omega_w)^2 c}{\gamma_0\gamma_{||}^2\Delta k^2 v_{||}^3}\beta_w\delta a\Phi[\sin\psi_0-\sin(\psi_0+\Delta kz) + \Delta kz\cos\psi_0] . \quad (33)$$

so that

$$\langle\sin\psi\rangle\simeq-\frac{c(\omega-\omega_w)^2}{2\gamma_0\gamma_{||}^2\Delta k^2 v_{||}^3}\beta_w\delta a\Phi \times[\sin(\Delta kz)-\Delta kz\cos(\Delta kz)] . \quad (34)$$

The small-signal gain over some length L is defined as

$$G_L\equiv\frac{\delta a(z=L)-\delta a(z=0)}{\delta a(z=0)} \quad (35)$$

subject to the requirement that $G_L\ll 1$. Substitution of Eq. (34) into Eq. (29) then yields

$$G_L\simeq\frac{\omega_b^2}{4c^2k}\beta_w^2\frac{(\omega-\omega_w)^2}{\gamma_0\gamma_{||}^2 v_{||}^2}\Phi\frac{1}{\Delta k^2} \times\int_0^L dz[\sin(\Delta kz)-\Delta kz\cos(\Delta kz)] , \quad (36)$$

which upon integration over z gives

$$G_L\simeq-\beta_w^2\frac{\omega_b^2L^3k}{16\gamma_0\gamma_{||}^2v_{||}^2}\left[\frac{\omega-\omega_w}{\omega}\right]^2\Phi\frac{d}{d\theta}\left[\frac{\sin\theta}{\theta}\right]^2 , \quad (37)$$

where $\theta\equiv\Delta kL/2$. Again, we observe that the small-signal gain [Eq. (37)] reduces to the expression found in the case of a magnetostatic wiggler.[13] The extrema occur for $\theta\simeq\pm1.3$ at which $d(\sin\theta/\theta)^2d\theta\simeq\mp0.54$, corresponding to frequencies

$$\omega\simeq\left[1-\frac{v_{||}}{c}\right]^{-1}\left[\omega_w+k_wv_{||}\left[1\mp\frac{2.6}{k_wL}\right]\right] . \quad (38)$$

Note that for $\Phi>0(<0)$, maximum gain occurs for $\theta\simeq1.3$ (-1.3); consequently, the effect of the axial-guide field is to cause a relative phase shift between the group I and group II ($\Phi<0$) classes of trajectories. In either case, however, the maximum gain is given approximately by

$$(G_L)_{\max}\simeq0.034\left[1+\frac{v_{||}}{c}\right]\beta_w^2\frac{\omega_b^2}{\gamma_0c^2k_w^2}(k_wL)^3 \times\frac{(\omega_w+k_wc)^2}{ck_w(\omega_w+k_wv_{||})}|\Phi| . \quad (39)$$

The resonant enhancement in both v_w and Φ due to the presence of the axial-guide field can result in substantial enhancements in the gain. As an example, we observe that in the absence of an axial-guide field $\beta_w\simeq0.052$ and $\Phi=1.0$ for the parameters shown in Figs. 2 and 3. This results in a gain of $(G_L)_{\max}\simeq3.69\times10^{-6}(k_wL)^3$. In contrast, $\beta_w\simeq0.53$ and $\Phi\simeq6.42$ when $\Omega_0/\gamma_0ck_w\simeq1.68$ near resonance. As a consequence, the gain is enhanced by several orders of magnitude and we find $(G_L)_{\max}\simeq(2.48\times10^{-3})(k_wL)^3$. A more detailed variation of the maximum gain as a function of the axial-guide field is shown in Fig. 4 in which we plot the maximum gain [normalized to the value of $(G_L)_{\max}$ for $B_0=0$] versus Ω_0/γ_0ck_w.

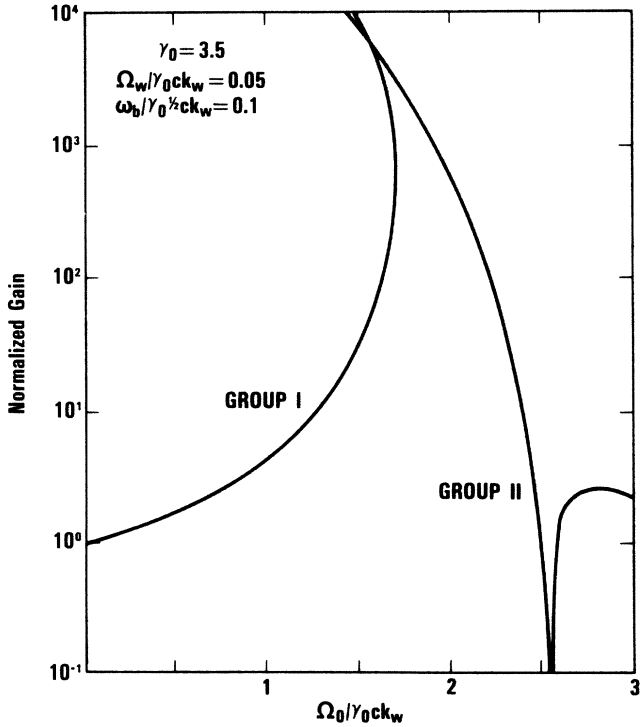

FIG. 4. Graph of the normalized gain versus the axial-guide field for $\Omega_w/\gamma_0ck_w=0.05$, $\gamma_0=3.5$, and $\omega_b/\gamma_0^{1/2}ck_w=0.1$.

IV. SUMMARY AND DISCUSSION

In summary, we have derived an expression for the small-signal gain for an amplifier configuration which consists of a large-amplitude electromagnetic wiggler field and an axial-guide magnetic field. Based upon a perturbation about a class of steady-state helical trajectories in the combined axial-guide and electromagnetic wiggler fields, a nonlinear pendulum equation has been derived which describes the axial bunching and trapping of electrons in the ponderomotive potential formed by the beating of the electromagnetic wiggler and the radiation field. It is important to observe, in this regard, that the natural response frequency of the electrons to a perturbation is given by $\bar{\Omega}$ which scales as

$$\bar{\Omega}\simeq\frac{1}{\gamma_0}[\Omega_0-\gamma_0(\omega_w+k_wv_{||})]+O\left[\frac{v_w^2}{c^2}\right] .$$

For sufficiently large axial fields, therefore, $\bar{\Omega}$ can become sufficiently small as to be comparable to the frequency of the ponderomotive wave. In this regime, the ponderomotive wave acts to drive the system near its natural frequen-

cy of oscillation, and a resonant interaction occurs which enhances both the ponderomotive potential and the gain. This resonance is described by the function Φ [Eq. (20)] which scales as $\bar{\Omega}^{-2}$. As a result, the expression for the gain displays a singularity at $\bar{\Omega}^2=0$, which coincides with the transition to orbital instability [Eq. (6)]. However, we have shown that the dispersion relation between the frequency and wave vector of the backwards-propagating electromagnetic wiggler [Eq. (8)] imposed by the dielectric response of the beam results in orbital stability. Hence, while the gain can be significantly enhanced, no singularity occurs within the context of the present model.

In contrast, Goldring and Friedland[9] calculated the gain under the assumption that the relation between the frequency and wave vector was externally determined (i.e., by a waveguide structure). All dielectric effects of the beam were neglected, and orbital instabilities were found for group I (II) orbits for a subluminous (supraluminous) wiggler. However, the expression obtained under this assumption does not appear to be equivalent to that derived herein [Eq. (37)] even if the condition in [Eq. (6)] were to be relaxed. As given by Goldring and Friedland, the gain exhibits singularities both at the transition to orbital instability ($\bar{\Omega}^2=0$) and at the point at which $dv_{\parallel}/d\gamma_0=0$ for the steady-state orbits. The singularity at the transition to orbital instability occurs due to the resonant enhancement in the ponderomotive potential discussed previously. However, the singularity occurring at $dv_{\parallel}/d\gamma_0=0$ is more difficult to understand and is not contained in Eq. (37). Finally, it should be remarked that in the limit of a magnetostatic wiggler $dv_{\parallel}/d\gamma_0=0$ occurs at precisely the point at which the $\bar{\Omega}^2=0$, and both gain expressions reduce to the well-known result for the small-signal gain in an idealized one-dimensional magnetostatic wiggler.

ACKNOWLEDGMENTS

This work was supported by the U.S. Office of Naval Research.

*Permanent address: Harry Diamond Laboratories, U.S. Army Laboratory Command, Department of the Army, Adelphi, MD 20783-1197.

[1]Y. Carmel, V. L. Granatstein, and A. Gover, Phys. Rev. Lett. **51**, 566 (1983).

[2]S. B. Segall, H. Takeda, S. Von Laven, and P. Diament, in *Free-Electron Generators of Coherent Radiation,* Proceedings of the Society of Photo-optical Instrumentation Engineers, Bellingham, WA, 1984, edited by C. A. Brau, S. F. Jacobs, and M. O. Scully (Society of Photo-Optical Instrumentation Engineers, Bellingham, WA, 1984), p. 178.

[3]J. Pasour, P. Sprangle, C. M. Tang, and C. Kapetanakos, Nucl. Instrum. Methods Phys. Res. **A237**, 154 (1984).

[4]P. Sprangle, V. L. Granatstein, and L. Baker, Phys. Rev. A **12**, 1697 (1975).

[5]P. Sprangle and A. T. Drobot, J. Appl. Phys. **50**, 2652 (1979).

[6]L. Friedland, Phys. Fluids **23**, 2376 (1980).

[7]H. P. Freund and P. Sprangle, Phys. Rev. A **28**, 1835 (1983).

[8]H. P. Freund, R. A. Kehs, and V. L. Granatstein, IEEE J. Quantum Electron. **QE-21**, 1080 (1985).

[9]A. Goldring and L. Friedland, Phys. Rev. A **32**, 2879 (1985).

[10]H. P. Freund and A. T. Drobot, Phys. Fluids **25**, 736 (1982).

[11]S. H. Gold, R. H. Jackson, R. K. Parker, H. P. Freund, V. L. Granatstein, P. C. Efthimion, M. Herndon, and A. K. Kinkead, in *Physics of Quantum Electronics,* edited by S. F. Jacobs, G. T. Moore, H. S. Pilloff, M. Sargent, M. O. Scully, and R. Spitzer (Addison-Wesley, Reading, Mass., 1982), Vol. 9, p. 741.

[12]P. Sprangle, C. M. Tang, and W. Manheimer, Phys. Rev. A **21**, 302 (1980).

[13]H. P. Freund, P. Sprangle, D. Dillenburg, E. H. daJornada, B. Liberman, Phys. Rev. A **24**, 1965 (1981).